Transport, Radiative, and Dynamical Effects of the Antarctic Ozone Hole: A GFDL "SKYHI" Model Experiment

J. D. MAHLMAN,* J. P. PINTO,** AND L. J. UMSCHEID*

*Geophysical Fluid Dynamics Laboratory/NOAA, Princeton University, Princeton, New Jersey
**U. S. Environmental Protection Agency, Research Triangle Park, North Carolina

(Manuscript received 1 March 1993, in final form 23 July 1993)

ABSTRACT

The GFDL "SKYHI" general circulation model has been used to simulate the effect of the Antarctic "ozone hole" phenomenon on the radiative and dynamical environment of the lower stratosphere. Both the polar ozone destruction and photochemical restoration chemistries are calculated by parameterized simplifications of the still somewhat uncertain chemical processes.

The modeled total column ozone depletions are near 25% in spring over Antarctica, with 1% depletion reaching equatorial latitudes by the end of the 4½-year model experiment. In the lower stratosphere, ozone reductions of 5% reach to the equator. Large coolings of about 8 K are simulated in the lower stratosphere over Antarctica in late spring, while a general cooling of about 1–1.5 K is present throughout the Southern Hemisphere lower stratosphere. The model atmosphere experiences a long-term positive temperature–chemical feedback because significant ozone reductions carry over into the next winter.

The overall temperature response to the reduced ozone is essentially radiative in character. However, substantial dynamical changes are induced by the ozone hole effect. The Antarctic middle stratosphere in late spring warms by about 6 K over Antarctica and the lower midlatitude stratosphere warms by approximately 1 K. These warming spots are produced mainly by an increased residual circulation intensity. Also, the Antarctic vortex becomes tighter and more confined as a result of the reduced ozone. These two dynamical effects combine to steepen the meridional slope of quasi-conservative trace constituent isolines. Thus, the entire transport, radiative, and dynamical climatology of the springtime stratosphere is affected to an important degree by the ozone hole phenomenon. Over the entire year, however, these dynamical effects are considerably smaller.

1. Introduction

A great deal of concern has been generated by the recent discovery of rapid depletion of total ozone over Antarctica during local spring (Farman et al. 1985). The total ozone mapping spectrometer (TOMS) on board *Nimbus-7* has provided areal coverage of its seasonal inception, development, and decay since launching in 1978. The satellite found depletions of total ozone over Antarctica as much as 50% compared to ground-based data taken during the 1960s. The satellite data also indicate that depletion of ozone may also be occurring at other latitudes in the Southern Hemisphere and at other times of the year. Both ground-based measurements and high-altitude aircraft flights have demonstrated that large concentrations of chlorine radicals derived from the photolysis of chlorofluorocarbons are likely responsible (Barrett et al. 1988; Anderson et al. 1989). Although much useful data have been collected for the morphology of the ozone hole and for elucidating possible mechanisms responsible for its formation, major questions still remain about the impact of the Antarctic ozone hole on the dynamics and thermal structure of the rest of the stratosphere.

The development of a stable wintertime polar vortex is a critical component for the initiation of ozone destruction in the Antarctic lower stratosphere during spring. When the dynamical forcing of the Southern Hemisphere stratosphere is weak, the polar vortex becomes very cold and isolated. Concomitantly, in such circumstances, the transport of chemical tracers into polar regions is strongly suppressed (Mahlman and Fels 1986). Moreover, such a strong polar vortex becomes quite resistant to erosion even when the dynamical forcing is increased (Juckes and McIntyre 1987). Therefore, variations in wintertime planetary-scale disturbance activity in the Southern Hemisphere troposphere (Mahlman and Fels 1986) need to be considered in determining the strength and stability of the south polar vortex. The importance of wave forcing to the zonal mean structure of the stratosphere of the Southern Hemisphere has been comprehensively discussed by Hartmann (1976a,b).

The lesser net dynamical heating of the Antarctic polar vortex relative to that of the Arctic causes the

Corresponding author address: Dr. J. D. Mahlman, USDC/NOAA/ERL/GFDL, Princeton University, Forrestal Campus, US Route 1, P.O. Box 308, Princeton, NJ 08542.

colder temperatures there, thus leading to its greater frequency of polar stratospheric cloud (PSC) formation. Heterogeneous reactions occur on the surfaces of the PSCs, converting chlorine in the relatively inert forms HCl and $ClONO_2$ (chemical lifetime of a few months) into more reactive Cl species, such as HOCl and Cl_2 (chemical lifetimes in sunlight of only a few hours). The sedimentation of PSC particles also removes gaseous HNO_3 from the system (Toon et al. 1986; Crutzen and Arnold 1986), preventing the formation of NO_2 and hence $ClONO_2$ in the springtime. Once the abundance of reactive nitrogen is reduced and the abundance of reactive chlorine is increased, rapid loss of ozone by chlorine can occur [for a concise review, see Solomon (1990)]. An as yet unquantified positive feedback loop between the chemistry of ozone destruction and dynamics is then established. This is because ozone loss leads to decreased solar heating and lower temperatures, resulting in a colder, more stable vortex and decreased downward transport of ozone into the vortex. This feedback mechanism also tends to increase interannual variability in ozone amounts, because small changes in one of these factors would be amplified by the other. The Antarctic ozone hole phenomenon thus provides a unique example of dynamical and chemical coupling, leading to very large ozone loss.

The dramatic ozone losses that have been observed might also be expected to impact the structure and circulation of the stratosphere. Kiehl et al. (1988) modeled the response of the high-latitude thermal structure to a prescribed ozone hole. Ozone depletions were derived from observations and not allowed to change in response to model motion fields. Their model was integrated from May to December to investigate the effects of ozone loss and the resulting decrease in solar heating on the stability and final breakup of the south polar vortex. They found cooling of about 5 K in October in the Antarctic lower stratosphere and a possible delay in the date of the final warming, compared to their control run. The model of Cariolle et al. (1990) shows similar results for local temperature anomalies during the duration of the ozone hole. Cariolle et al. (1990) and Prather et al. (1990) also included linearized chemistry to study the dispersal of ozone-poor air throughout the Southern Hemisphere. However, none of the studies mentioned above continued model integrations through winter of the following year. Longer integrations are needed to calculate the spread of ozone-poor air to the tropics and to the Northern Hemisphere, to calculate the accumulated depletion of ozone in the high-latitude stratosphere during successive annual cycles, and to assess the induced changes in stratospheric circulation.

The longer-term impacts of the Antarctic ozone hole on the thermal and dynamical structure of the entire stratosphere are not as easily discerned as the obvious short-term localized effects. The breakup of the polar vortex and subsequent spread of the ozone-poor air throughout the Southern Hemisphere result in much smaller perturbations to the local radiation budget than that occurring during Antarctic spring. Although the thermal signal may not be as dramatic throughout the year as during springtime, there is also the possibility that small but long-term changes in the mean thermal structure of the lower stratosphere could affect the stability and breakup of the Antarctic vortex during subsequent years. Any lasting alteration in the mean latitudinal thermal structure would also change the zonal-mean wind fields and, perhaps, the residual meridional circulation in the stratosphere. The importance of these possible feedback effects must be superimposed on the natural, interannual variability of the upward transport of tropospheric wave activity to the lower stratosphere. We have attempted to address several of these questions using the GFDL SKYHI general circulation model.

A summary of the features of the GCM, along with its successes and failures, is presented in section 2. We also discuss the experimental setup in this section. In section 3, we discuss the spread of the reduced ozone effects throughout the stratosphere, as well as the radiative and dynamical differences between the control and "ozone hole" model calculations.

2. Experimental design

a. Model background

Questions related to the impacts of the Antarctic ozone hole on the radiative and dynamical regimes of the stratosphere have been investigated through use of the SKYHI general circulation model developed at GFDL. The basic description of the model can be found in Fels et al. (1980). The model has 40 levels in the vertical, extending from the surface to about 80 km. The model is formulated in a vertical coordinate that is a modified terrain-following sigma system in the lower atmosphere and is identical to isobaric coordinates above 354 mb. The vertical grid spacing increases with height, from about 1.0 km in the middle troposphere to about 1.6 km at the 100-mb level and to about 2.7 km at the 1-mb level. The governing equations are discretized on a regular latitude–longitude grid. The present simulations use a grid spacing of 3° latitude × 3.6° longitude. Although the model can be run at various resolutions, we felt it desirable to perform these experiments at the highest resolution feasible in order to simulate as realistically as possible many of the features of the breakup of the Antarctic vortex. It was impractical to run the model at its improved, but experimental, 1° × 1.2° latitude resolution (Mahlman and Umscheid 1987) because of large demands in computer time. At this time, only two years of control simulation have been performed with the 1° × 1.2° latitude version.

Several aspects of the model's performance were initially summarized in Fels et al. (1980). There has been substantial improvement since that time, warranting a

description of new developments. A comparison of the SKYHI climatology, generated by six years of integration, with satellite data (Randel 1987) for the period 1979–86 indicate a number of areas of agreement and disagreement. In the lower stratosphere, the model winter temperatures over Antarctica are too cold by 5 K at 100 mb and 10 K at 50 mb. At higher levels, the model polar cold bias becomes much larger, reaching 40 K. Previously, Mahlman and Umscheid (1987) showed that the Northern Hemisphere polar cold bias is nearly eliminated in the 1° × 1.2° latitude SKYHI model, most noticeably above 10 mb. They showed that the discrepancy in the 3° × 3.6° latitude model is due to a dynamical forcing of the stratosphere that is too weak (see also Hayashi et al. 1989), relative to the high-resolution version. However, calculated mean temperatures agreed with observations to better than 5 K from January through March at high northern latitudes at all altitude levels in the stratosphere.

The dataset from Randel (1987) also included standard deviations of the monthly means over the seven years of the analysis. A comparison of model with observations revealed that interannual variability in temperature fields is simulated reasonably well by SKYHI. In the Southern Hemisphere at high latitudes, there is a tendency to underestimate the observed interannual relative standard deviation, with underestimates confined to less than 50%. In the Northern Hemisphere, the relative standard deviation of the zonal mean temperature is well simulated (to within 1 K at the 100-mb level, except for December and January, when again they were somewhat underestimated). It should be borne in mind, however, that this dataset also includes periodic adjustments to satellite retrieval routines and analysis methods. There is thus a question as to how much this has influenced the values. The model's systematic underestimation of interannual variability compared to observations is consistent with the decreased tropospheric wave activity forcing in the lower stratosphere in this version of SKYHI, compared to higher-resolution versions of SKYHI and reality (Mahlman and Umscheid 1987). This feature is directly related to the polar cold bias found in this version of SKYHI and other stratospheric general circulation models, but is noticeably improved by going to higher resolution (Mahlman and Umscheid 1987). Models that include additional ad hoc zonal momentum drag in the stratosphere can reduce the polar cold bias. However, these treatments are arbitrary in that neither theory nor observations are adequate for proper specification of these effects in models. We have elected to avoid such "tuning" parameterizations, so that ad hoc nonphysical distortions of the model's transport characteristics can be avoided.

b. *"Ozone hole" experiment*

After deriving the six-year control climatology for SKYHI, the model was then integrated for $4\frac{1}{2}$ years in an ozone hole model experiment as described below. Highly simplified chemistry, designed to simulate ozone destruction within the Antarctic vortex and subsequent photochemical restoration of ozone poor air transported out of the vortex, is included in this model experiment as described below.

At the time of this experiment, we lacked a complete, reliable, and self-consistent SKYHI 3D simulation capability for "background" stratospheric ozone. To allow investigation of some of the implications of the ozone hole phenomenon, we express the ozone mixing ratio (R) as

$$R = R_p - R'.$$

Here R_p is the prescribed ozone used in SKYHI based upon various ozone climatologies available in 1978 (Fels et al. 1980). The anomaly ozone R' is created by ozone hole destruction processes and is defined here as a *positive* quantity for convenience in modeling and interpretation. We then assume that the continuity equation for R_p is *independently* satisfied. Thus, in this model calculation only the R' equation is solved. However, the radiative transfer that drives SKYHI uses the *total* R, as defined above. The R' equation includes ozone sources and sinks, as described below, plus SKYHI's schemes for advection and diffusion of R' in response to the altered model circulation.

Many of the basic chemical processes for the initiation of ozone destruction during Antarctic springtime are inadequately known, most notably the details of the heterogeneous chemistry. Therefore, it is premature to attempt high-resolution simulations of a somewhat uncertain chemistry. However, we do wish to explore the impacts of polar ozone holes on the rest of the stratosphere and on the ozone hole formation process in subsequent years. We have thus developed a relatively simple scheme to initiate polar ozone destruction. The initiation of ozone destruction (chemical source of R') in SKYHI requires that three necessary conditions be met. Once all these local conditions are met, ozone destruction is initiated in the grid box. These conditions are based on a sufficient solar flux, desiccation of the air, and high local absolute vorticity of the air parcel. Within this framework, the ozone hole destruction of ozone (source of R') is parameterized by

$$\text{chemical source of } R' = + \frac{(R_p - R')}{30 \text{ days}} \delta_{\text{sun}} \delta_{H_2O} \delta_{\text{vorticity}}. \quad (1)$$

This "chemical source of R'" depends upon the complete ozone (R), because the destruction cannot continue after all the ozone ($R = R_p - R'$) has been destroyed. The 30 day e-folding time scale was chosen because it is roughly consistent with observed ozone hole destruction rates (Solomon 1990) but is specifically not "tuned" further in any way to reproduce observations. Because of the exploratory nature of this

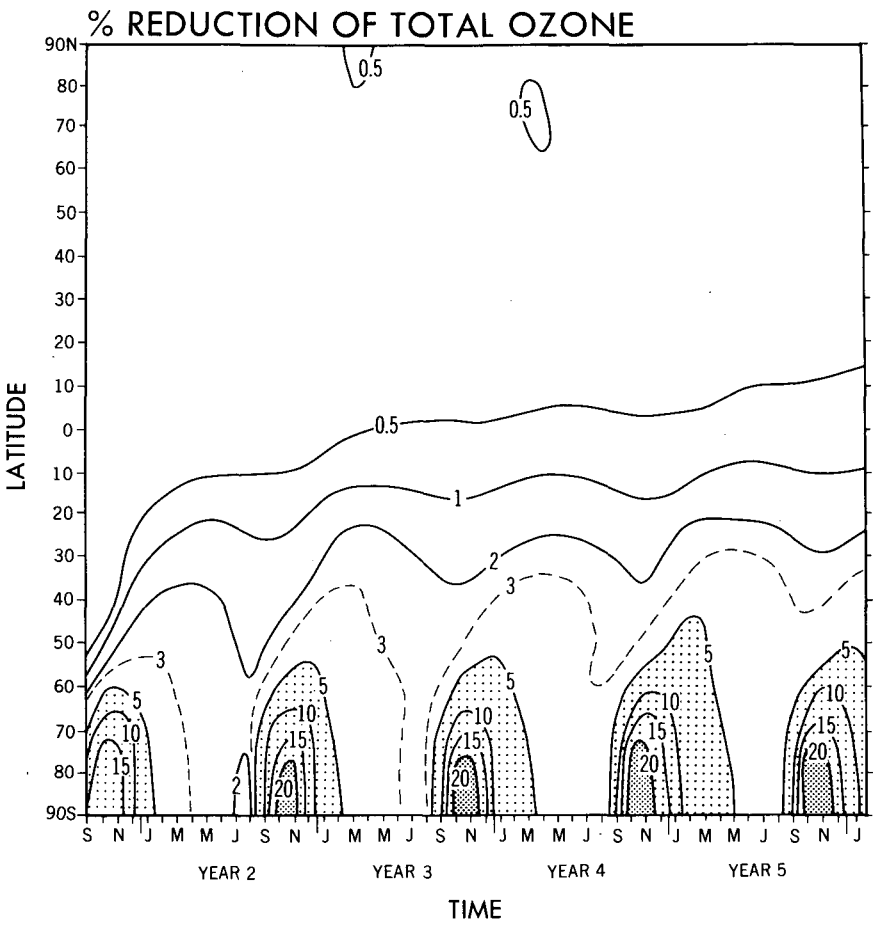

FIG. 1. Latitude dependence of percentage reduction in monthly, zonal mean total column ozone for the 4½ years of the "ozone hole" experiment, relative to the prescribed climatological ozone field used in the 6-year "control" SKYHI model experiment.

calculation, creation of a close match with observations for unphysical reasons is neither justified nor desirable. To initiate the chemical source of R' in Eq. (1), all three of the δ switches must be on. When a δ switch is "on," it has a value of one; otherwise, its value is zero.

The critical value for δ_{sun} in Eq. (1) is a noontime zenith angle less than 85°. This value is arbitrarily chosen to reflect the timing for the initiation of ozone destruction in accordance with observations. This switch thus permits ozone loss at the northernmost edge of the Antarctic vortex in the middle of September and allows ozone loss to occur at higher latitudes later as sunlight penetrates farther southward.

Results from the 1987 Airborne Antarctic Ozone Experiment (AAOE) campaign indicate that PSC particles are involved in ozone loss. The particles are presently thought to consist of two main types, nitric acid trihydrate (NAT) and water ice (Toon et al. 1986). The condensation temperature of NAT is about 192 K, and for water 185 K, for levels of gaseous H_2O and HNO_3 mixing ratios found in the winter Antarctic vortex (Toon et al. 1986). Water vapor is carried as a prognostic variable in SKYHI, and tends to condense in the cold Southern Hemisphere winter polar vortex. In SKYHI, the water amount condensed when grid box relative humidities exceed 85% is irreversibly removed as precipitation. Because the condensation temperature for water is several degrees lower than for NAT, desiccation of an air parcel ensures that denitrification has also occurred. To indicate desiccation of an air parcel, we have required that the local water vapor mixing ratio be less than 0.8 ppmv. This value is much lower than SKYHI's typical stratospheric water mixing ratios of ~1.6 ppmv. The choice of 0.8 ppmv for δ_{H_2O} thus requires a rather substantial desiccation of a parcel before the switch becomes activated. This choice may therefore lead to a model underestimation of the actual ozone losses. The SKYHI background stratospheric water amounts are too low because the model's equatorial tropopause is too cold in comparison to observations and no upper-stratospheric methane oxidation

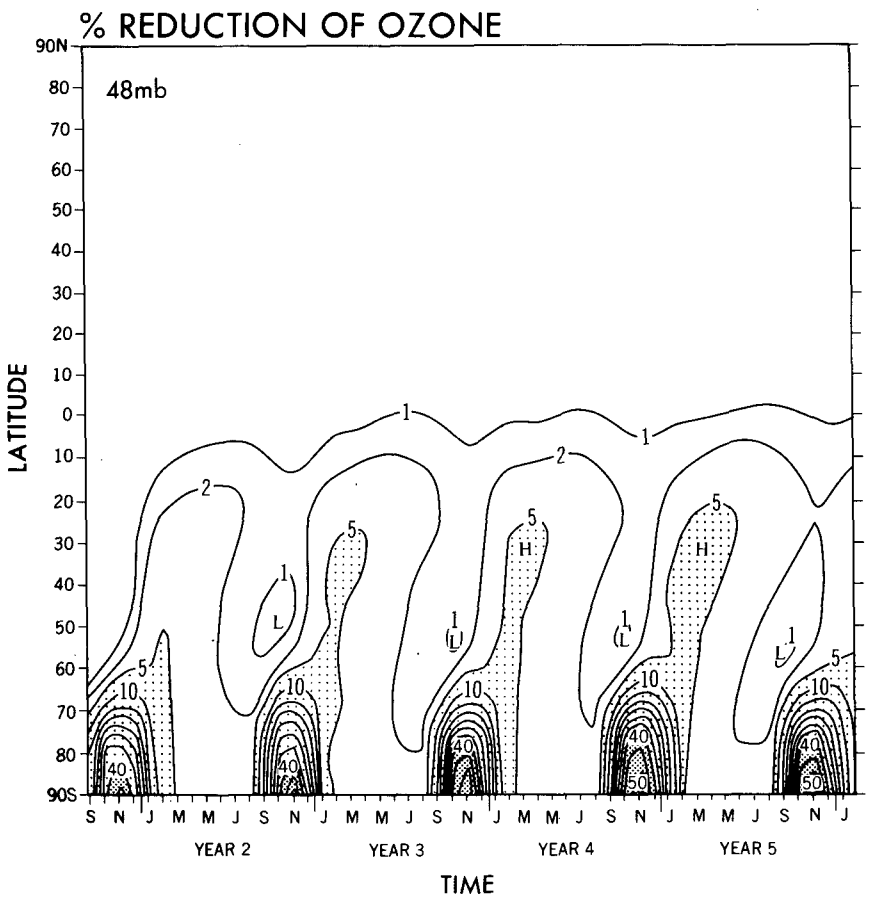

FIG. 2. As in Fig. 1 but for percentage reduction in ozone mixing ratio at 48 mb.

source of water is included in this version. This switch (δ_{H_2O}), once activated for a desiccated air parcel, remains on until outside air mixes in and restores the water vapor mixing ratio to a level greater than the critical value. This process thus mimics the renitrification of a denitrified air parcel through mixing in of nondesiccated air. This part of the parameterization is thus different from that of Cariolle et al. (1990), who activate this switch by a cold temperature (<195 K) criterion only. For denitrified and dehydrated air, our desiccation criterion seems more reasonable. If the odd nitrogen were to be sequestered rather than removed (presumably in relatively small NAT aerosol particles), a simple cold temperature switch may be reasonable because the reactive nitrogen can "pop back" once the parcel is warmed. We speculate that this type of sequestering process may be comparatively more relevant in the Northern Hemisphere where systematic removal through water ice is considerably less likely.

The critical value for water vapor can also be reached occasionally in the model near the tropical tropopause, thus potentially initiating ozone loss if this switch were to be triggered there. Such an equatorial ozone loss process would be physically unreasonable because such an air parcel would be virtually devoid of reactive chlorine or bromine, having come from the tropical troposphere. A substitute for the unavailable reactive chlorine was chosen in the form of the model's local absolute value of the absolute vorticity, since both quantities are characterized by large meridional gradients in the lower stratosphere. To ensure that a chemically active air parcel originates from a region of high absolute vorticity, we have required that the local absolute value be greater than twice the polar Coriolis parameter. By imposing this condition, ozone loss is confined to sunlit and desiccated polar air. These conditions thus allow ozone loss to continue in parcels torn away from the polar vortex until they are mixed with moister lower-latitude air. Note that this parameterization allows ozone loss to occur in higher latitudes of *either* hemisphere.

Once these three conditions are met, ozone destruction begins as prescribed in Eq. (1). This deliberately simplistic ozone destruction was arbitrarily limited to occur between the model's 103.6-mb and 12.2-mb surfaces. These model levels were chosen because the

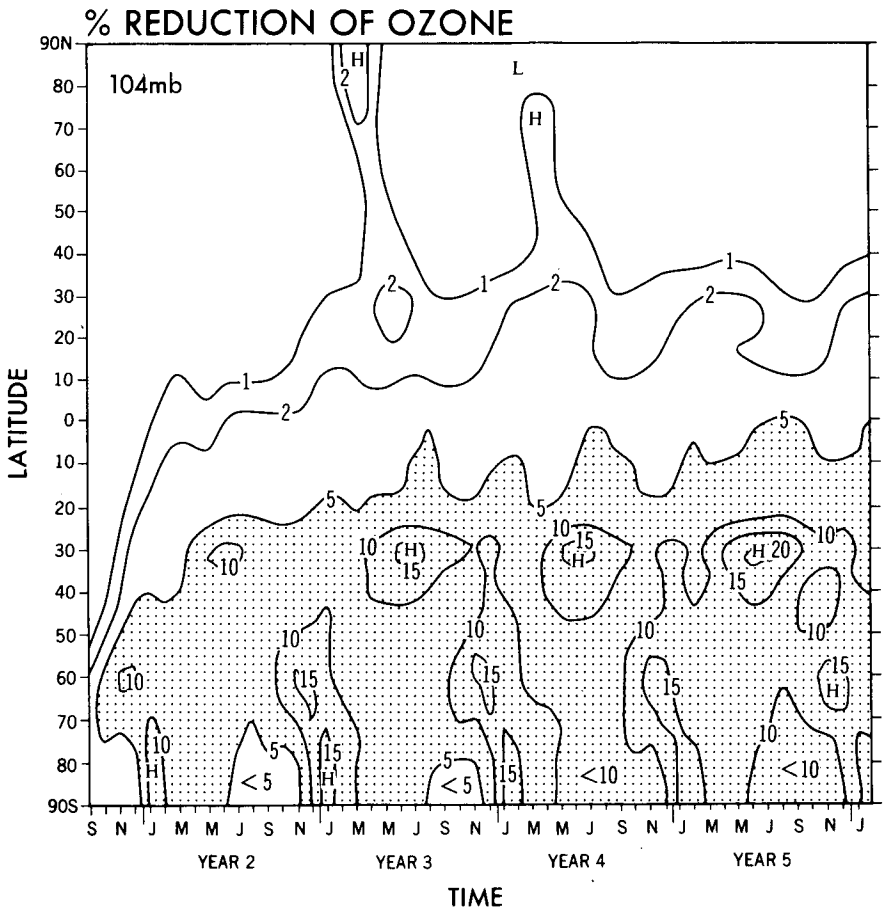

FIG. 3. As in Fig. 1 but for percentage reduction in ozone mixing ratio at 104 mb.

regions above and below these limits have not been observed to participate meaningfully in the polar ozone destruction process.

Once blobs of air are broken off from the vortex and transported globally, there must be some mechanism to allow for the photochemical restoration of the ozone-depleted air. For this model experiment, we have used a linearized chemistry to approximate the reformation of ozone in ozone-depleted air (chemical loss of R') parcels by a very simple scheme. The reformation parameterization used in this experiment is

$$\text{chemical loss of } R' = -2\, J^p_{O_2} R'/R_p. \qquad (2)$$

Here, $J^p_{O_2}$ is the total dissociation integral (including molecular oxygen density) for production of odd oxygen based upon precalculation from R_p, the prescribed model ozone. The parameterization thus restores the ozone anomaly by the rate at which background odd oxygen is formed, but scaled by the fractional perturbation R'/R_p. Values for $J^p_{O_2}$ are calculated using the treatment of Allen and Frederick (1982) in the Schumann–Runge bands. The absorption cross sections in the Herzberg continuum of O_2 are based on the measurements of Jenouvrier et al. (1986). The zonally averaged, height-dependent photolysis rates are calculated on a seasonal basis and time interpolated in the SKYHI model experiment. The ozone anomaly is thus restored rapidly in the "fast chemistry" regions where $J^p_{O_2}$ is large and is restored at a much slower rate in the lower stratosphere and at high latitudes where $J^p_{O_2}$ is small.

The chemical loss of R' given in Eq. (2) is only a rough approximation of the actual restoration rate. The true values can be obtained by performing a perturbation analysis about the SKYHI prescribed ozone values that are assumed to be in photochemical–*transport* equilibrium. In the high-latitude lower stratosphere, Eq. (2) can depart by as much as a factor of 10 from the true value, due to a dependence of the true value on the ratio of the prescribed ozone to the photochemical equilibrium value. However, this region is one in which the chemical restoration effect itself is extremely weak. In the "fast chemistry" region, where $J^p_{O_2}$ becomes large (fast restoration time), the expected error is always well less than a factor of 2.

Damping of ozone anomaly in the troposphere is accomplished by destruction in the bottom model level,

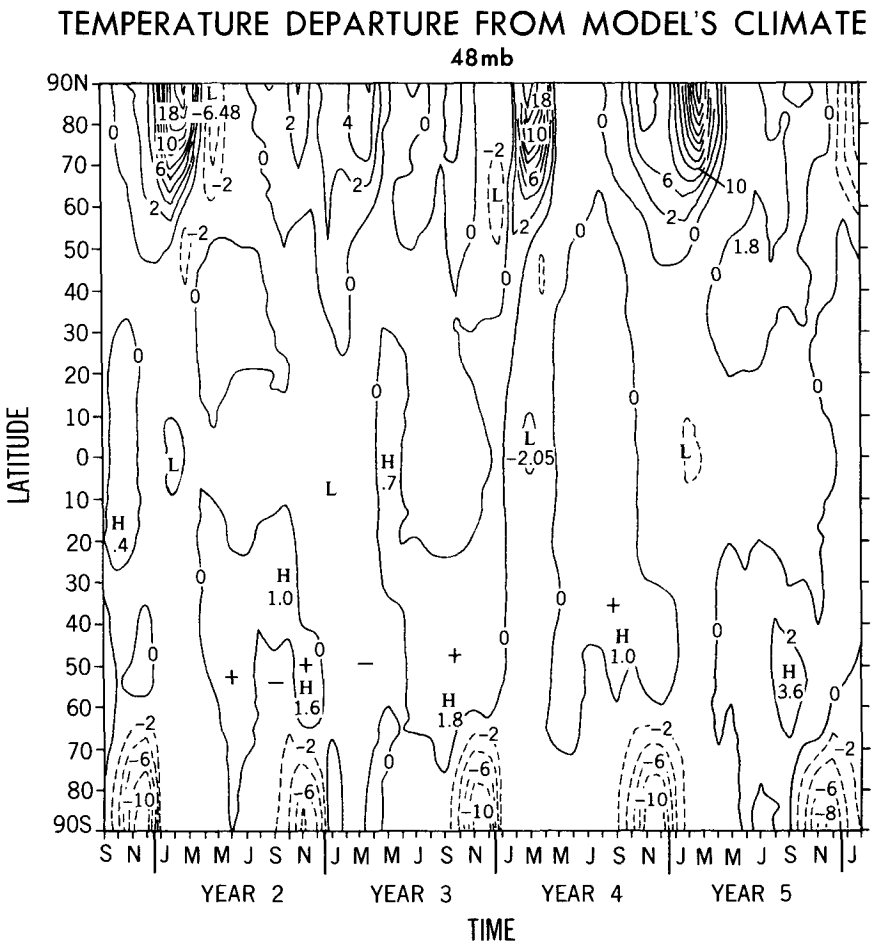

FIG. 4. Latitude–altitude distribution of monthly, zonal-mean temperature change (contour interval 2 K) for each month of the 4½ years of the "ozone hole" model experiment, relative to the 6-year mean monthly temperatures from the SKYHI control run.

using a deposition velocity of 0.1 cm s^{-1}. Although no chemical damping is included for the troposphere, the uptake by the surface is rapid enough to ensure that ozone anomaly injected into the troposphere is not significantly recycled into the stratosphere in tropical regions.

There are several consequences to be considered in adopting the anomaly approach versus a straightforward calculation of ozone itself. We have effectively ruled out the possibility of a contribution by transient upwelling to create an ozone hole (Mahlman and Fels 1986). This is because transport modification of the prescribed ozone field by the induced circulation changes is not included. The interannual variability in ozone amounts is thus underestimated because the only mechanism for producing it here is through generation and transport of ozone anomaly. The advantage of this approach, however, is that the effects of the ozone hole are isolated, the chemistry is substantially simplified, and the diagnostic analysis is more straightforward.

3. Model results

a. Simulation of reduced ozone effects

To simplify the interpretation, all results are expressed in percentage reduction from the prescribed model ozone climatology. Figure 1 shows percentage reduction of total ozone as a function of latitude and time for the 4½ years of the model experiment. Note that the simulated Antarctic zonal time average reduction exceeds 20%, with a tendency to grow with time. Each spring and summer shows a clear equatorward push of the reduced total ozone, followed by a retreat beginning in austral autumn due to transport being shut down and a temporary dominance of photochemical restoration.

Note that the 1% reduction line in Fig. 1 nearly reaches the equator and that the total ozone reduction has not leveled off, even by the end of the model experiment. The Northern Hemisphere 0.5% reductions are due to occasional activations of the ozone hole

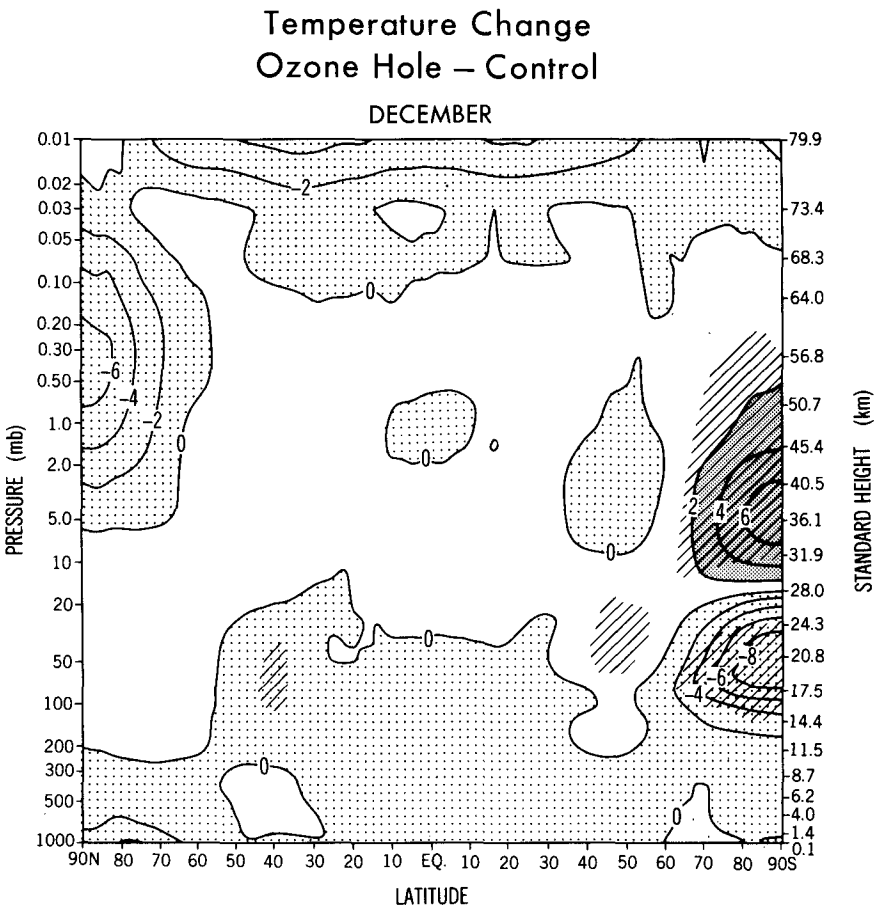

FIG. 5. December zonal-mean temperature change (contour interval 2 K) from 5-year December mean of the "ozone hole" experiment, relative to the 6-year December mean from the SKYHI control run. Hatched areas represent t test statistical significance exceeding 99%.

chemistry switch in late winter. The magnitudes of calculated ozone destruction there are very much smaller because the warmer and more dynamically active polar vortex in the SKYHI Northern Hemisphere late winter leads to higher polar water and lower polar vorticities for input to Eq. (1).

A crude comparison with observations is available through the observed trend in total ozone in percent per decade for the 1980s, as seen by the TOMS satellite (Stolarski et al. 1991). Since the onset of the ozone hole phenomenon occurred in the early 1980s, their ozone trend analysis provides a plausible baseline for interpreting the simulated results shown in Fig. 1. The observational record of Stolarski et al. (1991) shows maximum zonal time average polar reduction exceeding 30%, somewhat larger than this simulation. The equatorward penetration of the 2% line agrees well, while the lower values become lost in the statistical noise of their observations. The decay of ozone loss in midlatitude from late austral spring through winter is evident in both simulation and observations.

For the Northern Hemisphere, the result shown in Fig. 1 is very different from that of Stolarski et al. (1991). The TOMS data show surprisingly high ozone losses that are not captured by the model-determined ozone hole chemistry switch. This lends possible credence to recent hypotheses (e.g., Hofmann and Solomon 1989) that sulfate aerosol might catalyze a path for chlorine-related ozone destruction in midlatitudes. Another significant possibility is that the path of ozone destruction through the formation of NAT is dominant in the warmer Northern Hemisphere. That mechanism has not been included in the parameterized chemistry of our model experiment, because even its qualitative essence remains elusive. Finally, the temperature and water vapor biases of the model could be significant contributors to the discrepancy. Much further research will be required to answer this question.

Figure 2 shows the latitude–time evolution of 48-mb percentage reduction in model ozone mixing ratio. Its overall features are similar to the total ozone reductions of Fig. 1. Note that the magnitude of the late sum-

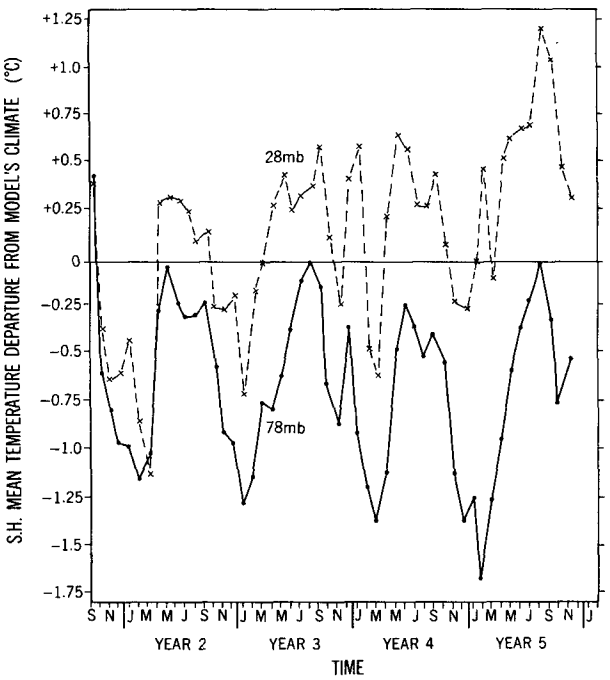

FIG. 6. Time evolution of monthly Southern Hemisphere mean temperature change for each month of the 4½ years of the "ozone hole" model experiment, relative to the 6-year Southern Hemisphere monthly mean temperatures from the SKYHI control run. Solid lines are for 78 mb and dashed lines are for 28 mb.

mer to late winter decreases in midlatitudes is much more pronounced than in Fig. 1. This is because the model's restoration chemistry becomes rather efficient on seasonal time scales at and above 50 mb in midlatitudes.

Note in Fig. 2 that the ozone hole tends to become deeper with time, as does the amount penetrating equatorward. The model's memory of the reduced ozone lasts into the next winter. This overall reduced ozone makes somewhat colder Antarctic winters than were present in the SKYHI control climate. This increases the number of events cold enough to initiate desiccation, and thus the parameterized ozone hole chemical loss.

Figure 3 shows latitude–time percentage reduction of model ozone mixing ratio at 104 mb. The structure here is very different from the total ozone and 48-mb structures seen in Figs. 1 and 2. The 1% reduction line has penetrated far into the Northern Hemisphere and the 5% line has reached the equator by the end of the model integration. The entire region and time interval shows pronounced trends in ozone reduction that are more evident than in either Fig. 1 or 2. Because the 100-mb level experiences little ozone hole chemical loss and little photochemical restoration, the reduced ozone there acts very much like a conservative tracer. The high-latitude peak in ozone reduction occurs in late spring and early summer due to downward transport from higher levels. The midlatitude winter peak in ozone reductions (up to 20% by year 5) is caused by the onset of the mean winter descending motion in midlatitudes bringing reduced ozone to the lower stratosphere.

b. Impact on stratospheric thermal structure

A major goal of this work is to understand the impact of the ozone hole on the overall climatology of the stratosphere. The main path through which this can occur is through the role of ozone as a radiatively active trace gas.

Figure 4 shows latitude–time differences at 48 mb between the monthly zonal mean temperatures in the ozone hole experiment and a 6-year mean of the SKYHI control run. Figure 4 shows at 48 mb that large cooling, ranging from 6 to 10 K, is prevalent near the Antarctic region. Note that there is a suggestion of warming in nonpolar latitudes in November and December, with a maximum at 50°–60°S. In winter northern polar regions, large warming and cooling events are evident. There is no evidence that these events are in any way caused by the imposition of ozone hole effects. These large anomalies vary from year to year and from month to month in a nonsystematic manner. This is a region and time in which the interannual variability is high due to the highly active planetary wave dynamics of the winter Northern Hemisphere.

Figure 4 also shows a weaker polar cooling and a stronger warming near 50°S in the austral spring of year 5. This indicates that a stronger dynamical forcing during this year acted to warm the higher-latitude regions more than usual.

The above results raise a number of questions concerning the temperature changes due to the influence of the ozone hole. To what degree are the changes statistically significant, and are those changes due to direct radiative effects or to an indirect dynamical mechanism?

Figure 5 presents the average temperature difference for December between the five Decembers of the ozone hole experiment with 6 years of the SKYHI control run. The Antarctic lower stratosphere shows strong cooling with values exceeding 8 K. Remarkably, a warming of 6 K occurs near 30–40 km over Antarctica and a warming of 1 K is found near 50°S in the lower stratosphere. Note that both warming and cooling show statistical significance (areas enclosed by hatching) exceeding 99%, frequently exceeding 99.9%, as calculated by a standard Student's t-test. Consistent with this cooling, the analysis shows a zonal wind increase of greater than 10 m s^{-1} for December (15 m s^{-1} for November) at 70°–80°S above 20 km that is significant at the 99.9% confidence level. The statistically significant warming above and outside the ozone-induced cooling in the ozone hole region is caused mainly by an induced increase in the higher-latitude descending branch of the

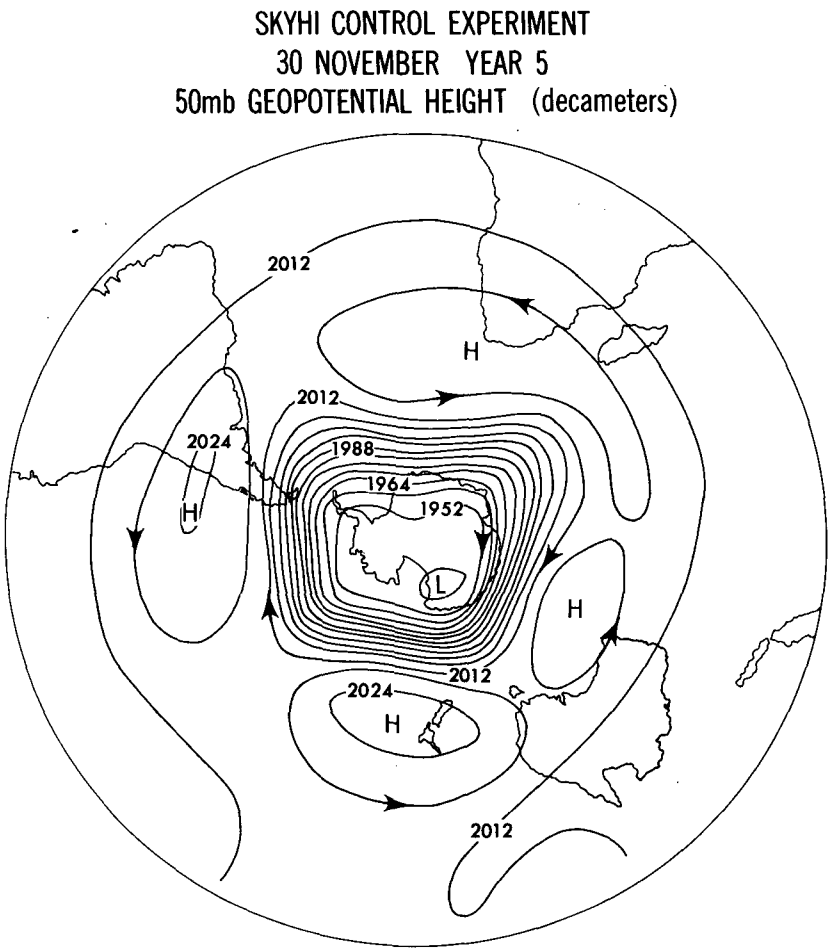

FIG. 7. The 50-mb geopotential height (decameters) chart for 30 November year 5 from the SKYHI control model experiment.

model's residual meridional circulation. However, the radiative transfer model of Shine (1986) predicts several degrees of warming in a shallow layer just above the depleted ozone. This effect contributes to the warmed layer seen in Fig. 5, but the simulated effect is considerably deeper and larger than can be explained by radiative changes only. The cooling in lower latitudes appears to be in part due to the ascending branch of this altered residual circulation. There are many similarities between the temperature responses noted here and the shorter exploratory model studies by Kiehl et al. (1988) and Cariolle et al. (1990).

The observational data in Randel (1987) shows a similar temperature change structure for the 1987 ozone hole event, with the strongest signal appearing in October and November. In our model experiment, the stronger signals are for the months of November and December. This is consistent with the polar cold bias of the model, which generally acts to delay the onset of the spring warming by 2–3 weeks, relative to observation. This t test also suggests that a cooling is present near 100–50 mb at 40°N at the 99% confidence level. This spot is not thought to be physically significant, since it does not appear in equivalent calculations for November or January. The high cooling near the Northern Hemisphere high latitudes near 50–60 km or at 75–80 km in the Northern Hemisphere is not statistically significant because of the very large model winter interannual variability there.

Figure 5 also suggests cooling in much of the troposphere, although it is not calculated to be statistically significant at the high confidence interval used here. Over the 70°–90°S region, the upper-troposphere cooling appears to be a significant effect in the model. This is in qualitative agreement with radiative expectations due to the reduced temperatures in the lower stratosphere (Ramaswamy et al. 1992). The colder temperatures reduce the downward infrared flux to the troposphere. All other things being equal, tropospheric cooling should occur, but it is expected to be muted in this model due to its use of prescribed sea surface temperatures. A quantitative answer to that question is be-

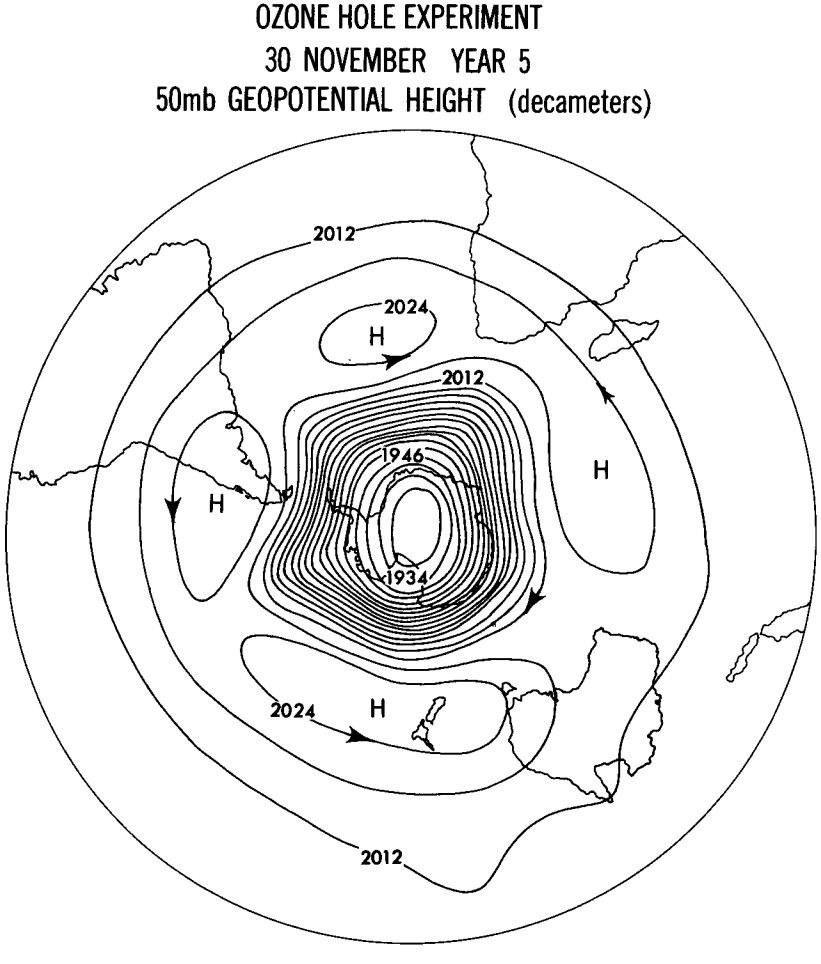

FIG. 8a. The 50-mb geopotential height (decameters) chart for 30 November year 5 from the SKYHI ozone hole experiment.

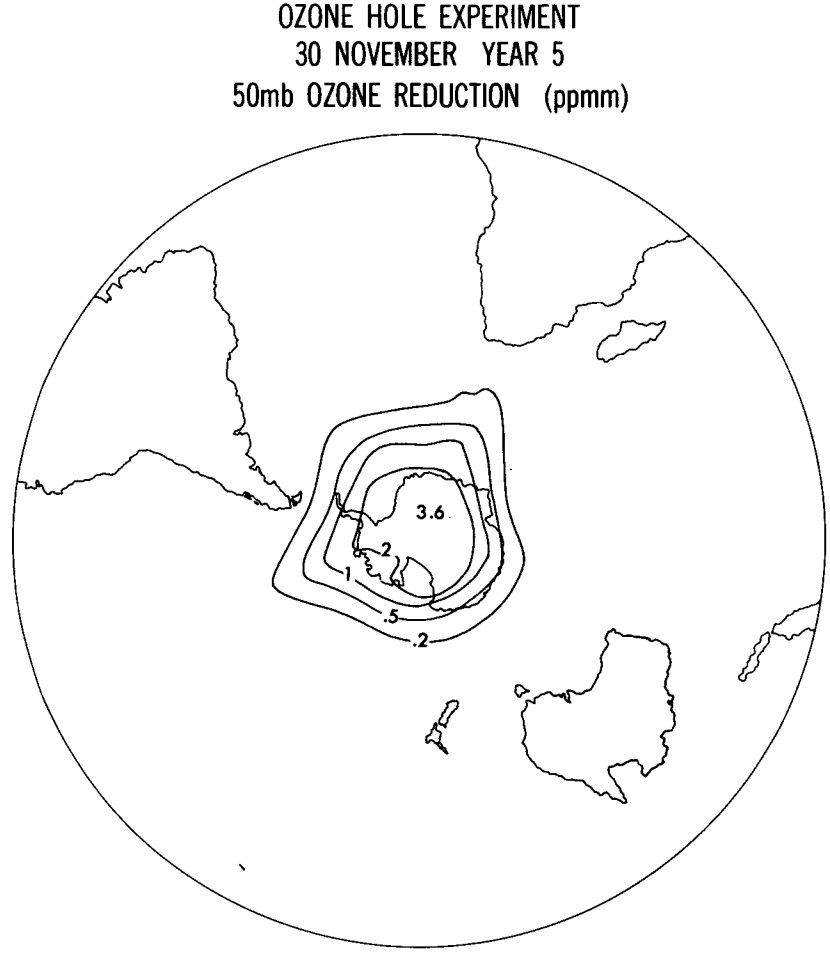

FIG. 8b. The 50-mb ozone mixing ratio reduction (ppmm) chart for 30 November year 5 from the SKYHI ozone hole experiment. Ozone reduction is the loss in ppmm relative to the SKYHI control prescribed ozone climatology.

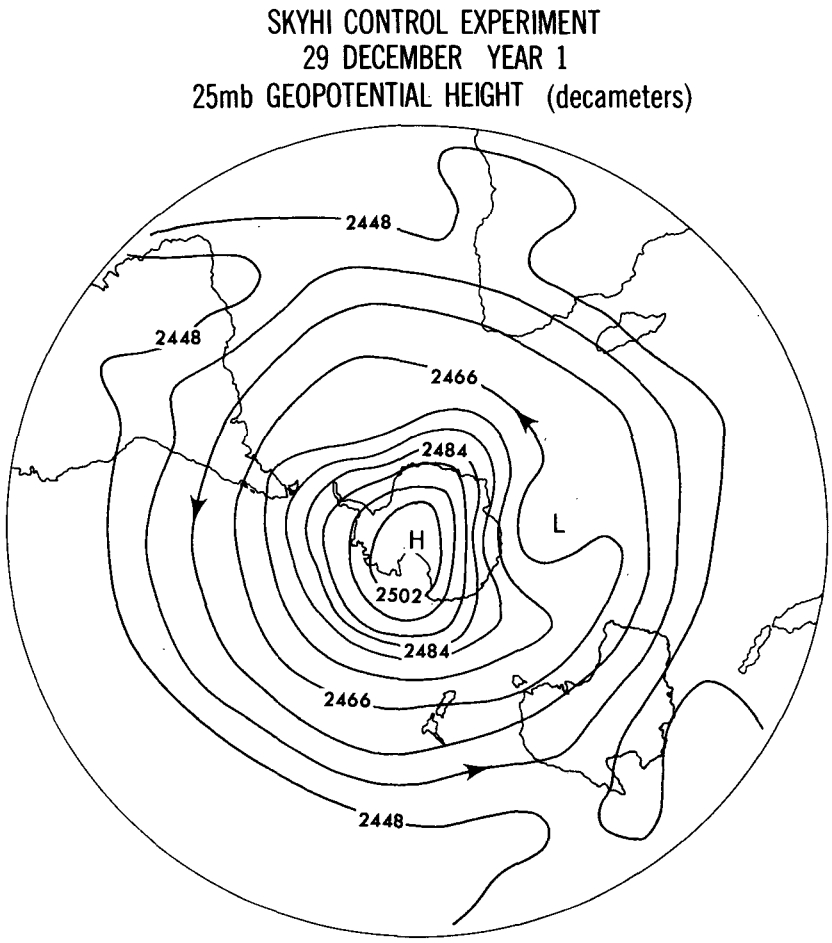

FIG. 9. The 25-mb geopotential height (decameters) chart for 29 December year 1 from the SKYHI control experiment.

yond the scope of this paper, but is under current active investigation.

With the onset of the Southern Hemisphere summer season, the large polar temperature change signals shown in Fig. 5 disappear. Interestingly, the 50–100 mb region between 20° and 80°S shows systematic coolings of 1 to 1.5 K that are statistically significant at the 99.9% confidence level for the months of January, February, and March. This systematic cooling signal is radiatively consistent with the meridional spreading of reduced ozone seen in Figs. 2 and 3. Widespread coolings of 0.5 to 1 K are also seen at 20°N–20°S at 50–100 mb and in the Antarctic upper troposphere, but are not judged to be statistically significant at the 99% level, given our limited sample of model years.

Figure 6 shows the time evolution of the Southern Hemisphere mean temperature change for the ozone hole experiment minus the 6-year SKYHI control. The bottom curve is for 78 mb, a level in the middle of the greatest ozone reductions, while the top curve is for 28 mb, a region considerably less affected because of the much faster photochemical ozone restoration there. Note that the 78-mb level shows a substantial seasonal signal, with the largest decreases appearing in the December–March period. This record shows a gradual cooling through the length of the model experiment. By year 5, the largest hemispheric mean cooling exceeds 1.5 K, with an annual mean cooling of nearly 1 K. This is generally consistent with the annual mean 100–50-mb levels of cooling found by Oort and Liu (1993) from the radiosonde record for the 1980s. Interestingly, their observational analysis suggests a smaller seasonal cycle for this change than does this model experiment. The upper plot in Fig. 6 for 28 mb shows a small net Southern Hemispheric mean warming with nonperiodic and seasonal fluctuations that are similar to those at 78 mb. These nonsystematic fluctuations are roughly consistent with fluctuations in the difference between the hemispheric mean compression heating for the ozone hole experiment and the model control (not shown).

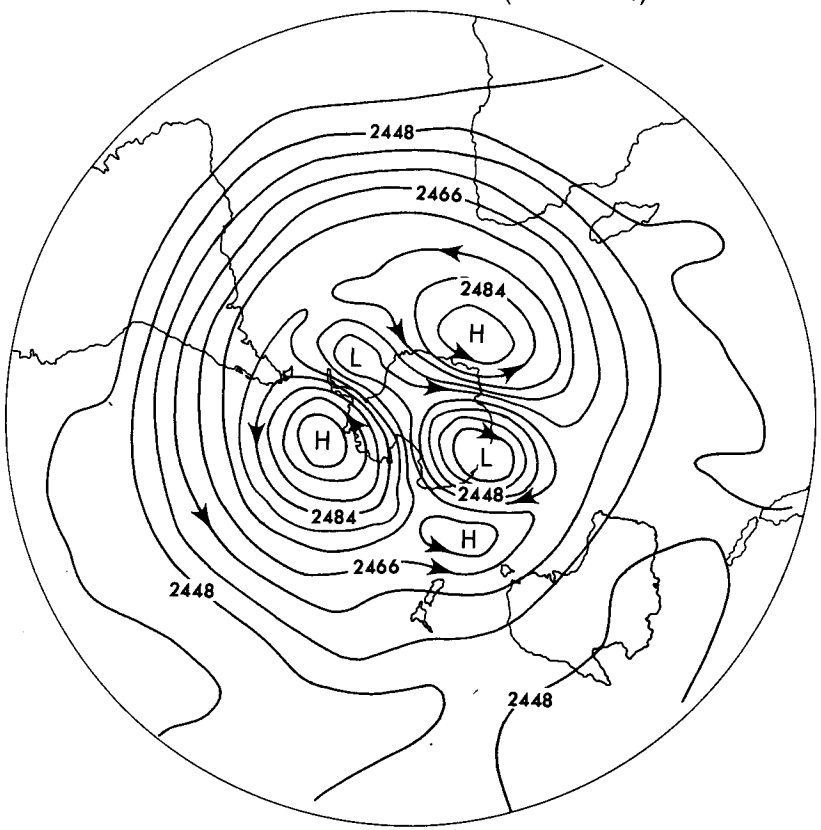

FIG. 10a. The 25-mb geopotential height (decameters) chart for 29 December year 1 from the SKYHI ozone hole experiment.

FIG. 10b. The 25-mb ozone mixing ratio reduction (ppmm) chart for 29 December year 1 from the SKYHI ozone hole experiment.

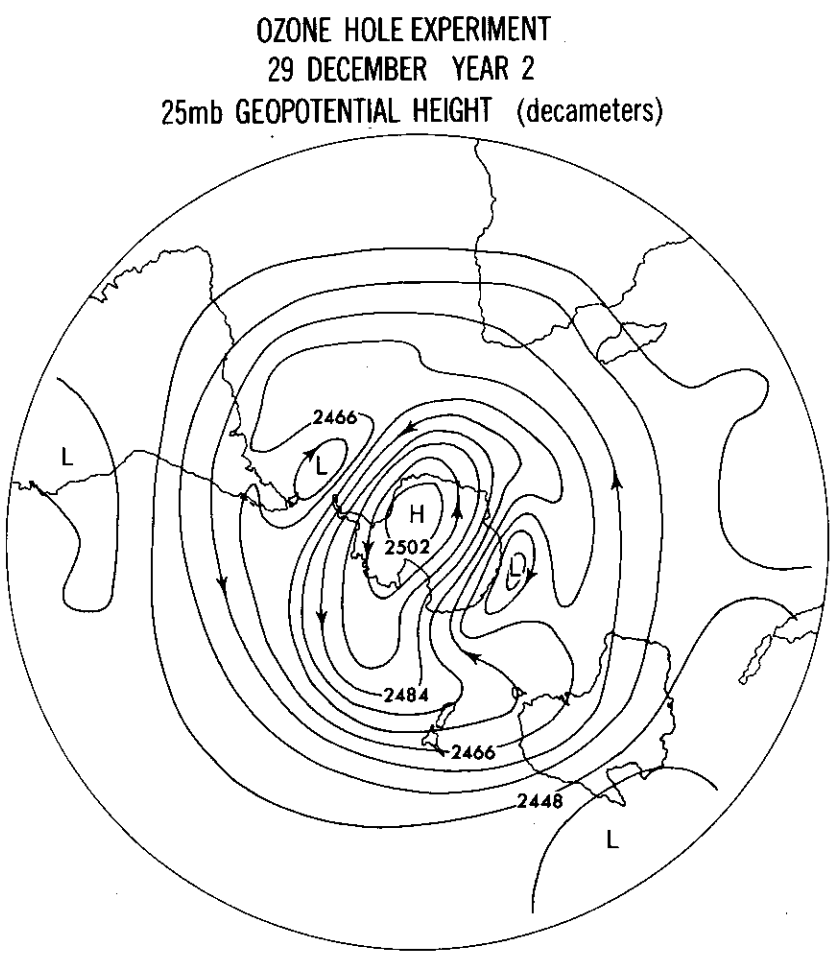

FIG. 11a. The 25-mb geopotential height (decameters) chart for 29 December year 2 from the SKYHI ozone hole experiment.

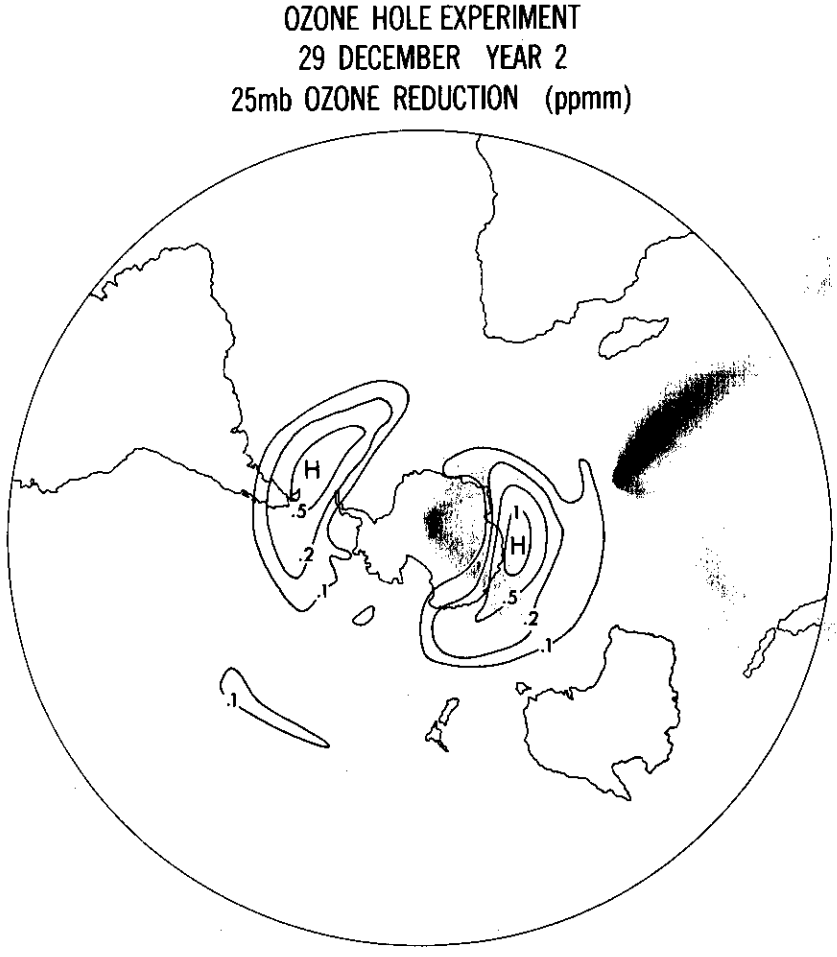

FIG. 11b. The 25-mb ozone mixing ratio reduction (ppmm) chart for 29 December year 2 from the SKYHI ozone hole experiment.

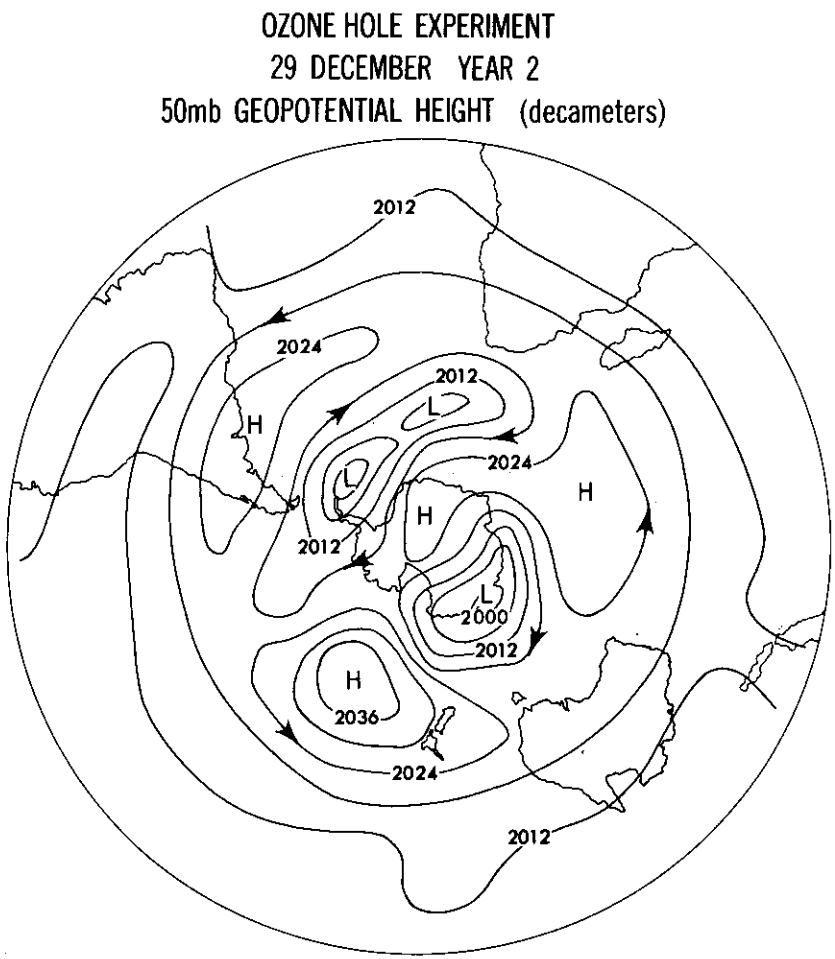

FIG. 12a. The 50-mb geopotential height (decameters) chart for 29 December year 2 from the SKYHI ozone hole experiment.

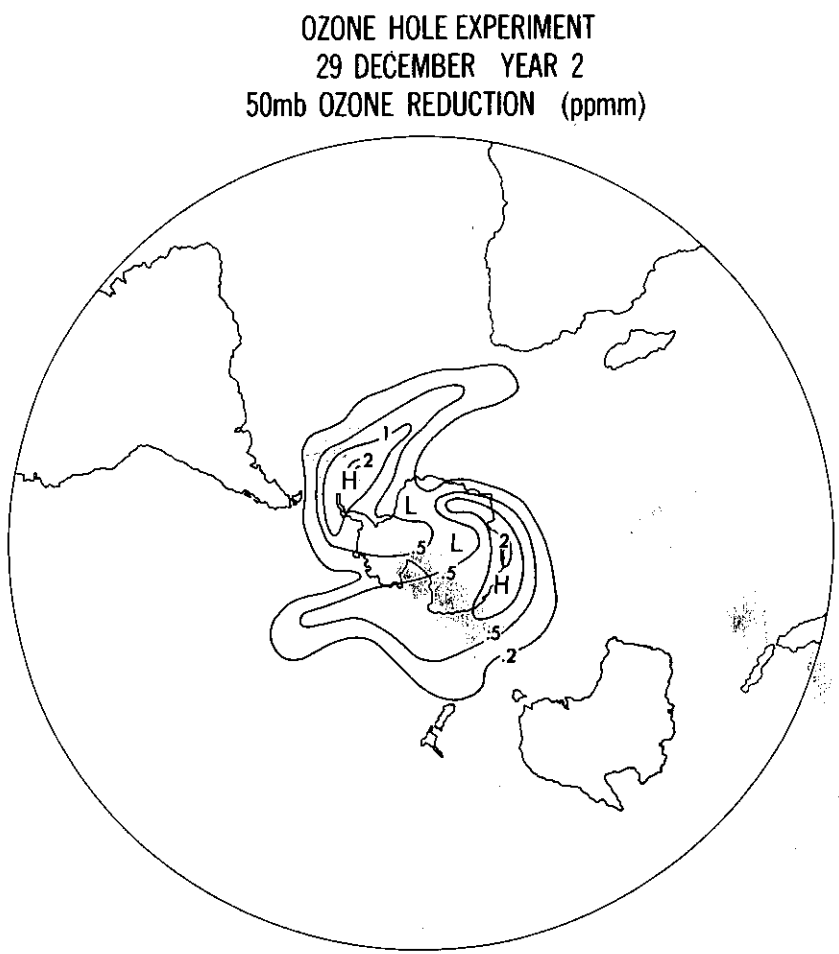

FIG. 12b. The 50-mb ozone mixing ratio reduction (ppmm) chart for 29 December year 2 from the SKYHI ozone hole experiment.

FIG. 13b. The 100-mb ozone mixing ratio reduction (ppmm) chart for 29 December year 2 from the SKYHI ozone hole experiment.

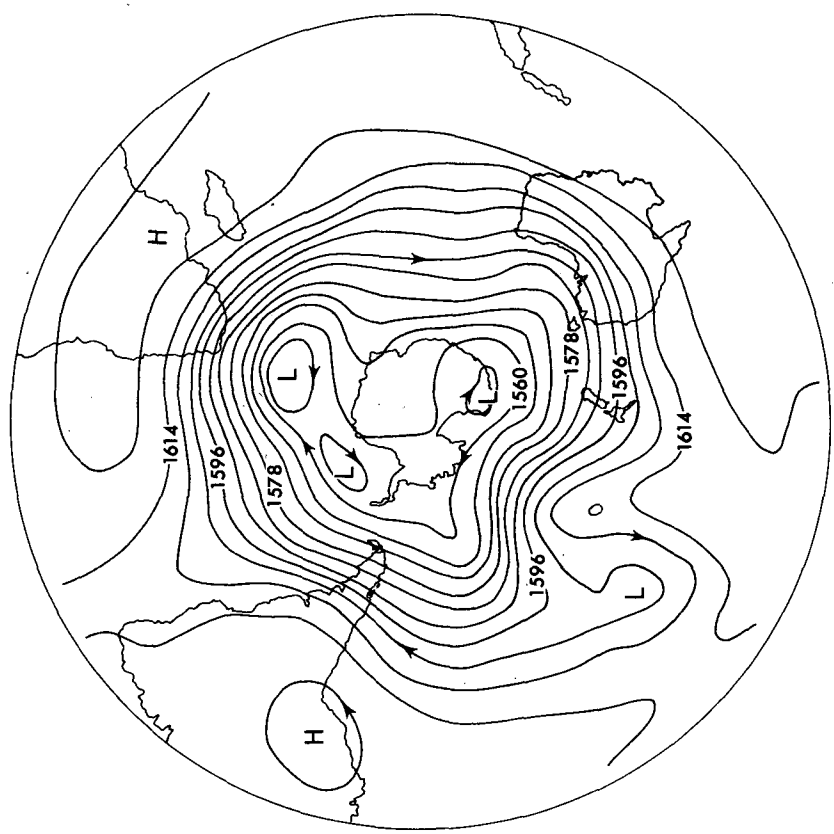

FIG. 13a. The 100-mb geopotential height (decameters) chart for 29 December year 2 from the SKYHI ozone hole experiment.

All of these results demonstrate the large impact that ozone hole destruction chemistry has on the thermal structure of the lower stratosphere. Another robust effect appears as a delay in the rapid seasonal warming that takes place in Antarctic latitudes between September and January. A simple way to evaluate this is to compare the mean geopotential height changes between the ozone hole experiment and the control for a given month mean with the monthly changes in the control. From 104 to 21 mb, the ozone hole experiment geopotential height changes are about one-third of the month-to-month changes in the control. Thus, crudely speaking, the climatic effect of the model's reduced polar ozone is to suppress the onset of the springtime filling of the polar vortex by about 10 days.

c. *Radiative versus dynamical response to altered ozone*

Several investigators [most notably Shine (1986)] have made direct radiative calculations from the Antarctic ozone decreases by invoking the so-called fixed-dynamical heating (FDH) approximation (Fels and Kaplan 1975). This concept was developed to investigate the relevance of "inspired" radiation-only calculations in the context of climate change due to changed atmospheric constituents. Here we simply write the thermodynamic equation as

$$\frac{\partial T}{\partial t} = Q_{\text{rad}} + Q_{\text{dyn}}, \tag{3}$$

where Q_{rad} is the net radiative heating and Q_{dyn} is the net heating due to all dynamical processes (compression, advection, diffusion).

Extending the FDH approximation for a transient climate change, we write

$$\frac{\partial \Delta T}{\partial t} \approx \Delta Q_{\text{rad}}. \tag{4}$$

This transient form of the FDH approximation thus neglects the *change* in the dynamical heating, that is, that part of the heating due to the changed atmospheric circulation that resulted from the changed constituents. Fels et al. (1980) showed that the standard FDH approximation works rather well when applied in an extratropical, annual mean context, but failed noticeably in the tropics.

To what degree is non-FDH behavior relevant in a seasonally transient high-latitude situation such as described here? Part of the answer is already evident in the discussion describing Figs. 3, 4, and 5. Warming occurs in late spring at midlatitude locations where the ozone and thus the net radiative heating have actually decreased.

The adjustment resulting from changed ozone can be seen more clearly through detailed examination of the changed thermodynamic balance of Eq. (3) for the control minus the ozone hole model experiments. This analysis shows that the initial response to the reduced ozone is a sharp reduction of the rate of seasonal warming, mostly due to reduced solar heating. By November, however, the temperature tendencies in the control and ozone hole experiments are very similar. The net radiative heating has decreased in high latitudes by about 0.2° day^{-1}, while the net dynamical heating (mainly compression heating) has increased by a comparable amount. The analysis shows that the changed circulation required to support this is hemispheric in scale with the largest positive (sinking) changes near Antarctica. The negative (rising) changes begin equatorward of 50°S, are smaller in magnitude, and cover a broader area. These results indicate that the entire Southern Hemisphere residual meridional circulation has increased in intensity. This agrees in essence with the inference of Kiehl et al. (1988) based upon a GCM experiment that invokes a prescribed ozone hole and a single season's integration. Because dynamical heating varies considerably from year to year, multiple year integrations are required to establish this point clearly. The high-latitude downward residual meridional circulation has increased in intensity during this seasonal transition by about 0.6 km month^{-1}.

This circulation change is large enough to affect the climate and the transport characteristics of the entire Southern Hemisphere stratosphere. It is fair to say, however, that the effect becomes rather small upon averaging over the entire course of the year. This analysis is thus consistent with the tentative conclusion of IPCC (1992), that the overall climatic response to Antarctic ozone losses is essentially radiative in character.

d. *The ozone hole and breakup of the South Polar vortex*

Since the ozone-depleted region under investigation is created within the late winter polar vortex, the spread of this air to other latitudes is fundamentally related to the erosion and destruction of this vortex. It is also of primary interest to determine the degree to which the structure of the polar vortex itself (and its associated transport properties) is affected by the substantial ozone depletion. We offer here some preliminary results that provide considerable insight into these processes.

Figures 7 and 8a show 50-mb geopotential height charts for the day 30 November in year 5 of the "control" and "ozone hole" experiments, respectively. The two instantaneous charts are quite representative of the mean differences between the two model experiments. The ozone hole geopotential height chart of Fig. 8a has a vortex minimum that is about 180 m deeper than that of the control in Fig. 7. Figure 8b gives the amount of 50-mb ozone reduction (ppmm) in the same 30 November year 5 date of the ozone hole experiment. This figure shows that most of the ozone-depleted air is still tightly confined within the cyclonic polar vortex at this time.

Figure 9 shows the 25-mb control geopotential height chart for 29 December year 1 and reveals a summertime pattern with a polar anticyclone and relatively weak easterly flow. Figures 10a and 10b show the 25-mb ozone hole geopotential height and ozone reduction, respectively, for 29 December year 1. The dramatic contrast in the height field between Figs. 9 and 10a illustrates the tendency of the reduced polar ozone to help maintain the polar vortex against the rapid radiative destruction at this time of year. Figure 10b illustrates the point by revealing that the ozone-depleted air is still mostly confined within the (now distorted) cyclonic vortex.

Figures 11a and 11b show the same height and ozone reduction fields as Figs. 10a and 10b but for year 2, a year later. In this more dynamically active year (compare year 1 and year 2 Decembers in Fig. 4), an anticyclone has just penetrated the polar cap and has split the ozone-reduced air into two cyclonic pieces well off the pole. Figures 11a and 11b demonstrate convincingly that the model's "final warming" results from a dynamic replacement of the polar air, rather than by a simple radiative destruction of the polar vortex at the onset of summer.

Figures 12a and 12b are for the same fields and date as Figs. 11a and 11b but for 50 mb. Here, the geopotential height field is more complex because of its lingering "memory" of tropospheric disturbances. Note, however, that anticyclones are also penetrating the polar region, accompanied by an associated "fanning out" of the ozone-depleted air into lower latitudes. The impact of this process on the zonal-mean behavior is clearly evident in Fig. 3. The breakup destroys the low polar ozone region and spreads it into tropical latitudes over the next few months.

Figures 13a and 13b show the same fields as Figs. 11 and 12 but for 100 mb. Here, as in the real world, the polar vortex boundary is much less clearly defined. Because of this, the ozone reduction of Fig. 13b is more spread out than at the higher levels in Figs. 10b, 11b, and 12b. As the model progresses into the summer season, however, the meridional spreading of the reduced ozone is much more pronounced at higher levels, because the flow reverses to easterlies at 50 mb and above. The effect of this difference can be seen by comparing the evolution in Figs. 2 and 3 in January and February. A complicating factor in this interpretation is that most of the model's reduced ozone at 100 mb is transported there rather than produced there.

e. Impact of the ozone hole on stratospheric transport

In the above two sections, we have identified two distinct dynamical responses of the stratosphere to the reduced Antarctic ozone. In section 3c, we noted an increased intensity of the descending diabatic circulation in higher latitudes. Section 3d revealed a noticeable "tightening" of the polar vortex that reduces the rate of horizontal mixing of air across the vortex boundary.

These two results can be interpreted in terms of the mechanistic "equilibrium tracer slopes" model of Mahlman et al. (1986). In this framework, the meridional slope of a quasi-conservative constituent isoline is determined, to first order, by an approximate balance of the slope-steepening effect of the diabatic meridional circulation and the slope-flattening effect of wave-induced meridional mixing. In this model experiment, the transient springtime response to the onset of the reduced Antarctic ozone is a steepening of the meridional isoline slopes of *all* longer-lived trace constituents. Thus, the entire transport climatology of the Southern Hemisphere stratosphere has been altered by the Antarctic ozone destruction. This effect is pronounced in the springtime, but becomes much less significant if annual mean or hemispheric mean processes are being considered. Put another way, the use of fixed dynamical heating radiative models to examine annual mean climatic responses to altered stratospheric ozone is a reasonable simplification in spite of this noticeable dynamical effect, as was tentatively concluded in IPCC (1992).

4. Conclusions

The GFDL "SKYHI" general circulation model has been used to simulate the transport, radiative, and dynamical effects of the Antarctic ozone hole phenomenon. A simple, but physically plausible, parameterization of the ozone hole destruction chemistry is included, as well as a parameterized photochemical restoration of the reduced ozone. The model was run for $4\frac{1}{2}$ years in the "ozone hole" experiment, with the results being compared to 6 years of SKYHI model "control" climatology.

The model results show substantial meridional spreading of the reduced ozone, seasonally and progressively over time. The total column reductions range from near 25% in Antarctic October and November to near 1% in equatorial regions. This model simulation compares favorably to observed total column depletions over the decade of the 1980s (Stolarski et al. 1991). In the lower stratosphere near 100 mb, the depletions are much less confined to polar regions, while reductions near 5% are simulated near the equator.

The model experiences a long-term positive feedback through the reduced ozone amounts carrying over into the next winter. This produces a progressively colder high-latitude lower stratosphere, thus enhancing the likelihood that ice clouds will be formed in subsequent years. It is possible that this memory effect has played some role in the recent near disappearance of the earlier tendency of the ozone hole to appear in alternate years.

The time-averaged temperature response relative to the model's control climatology shows large lower

stratosphere cooling (~8 K) near the pole in December. The model experiences polar *warming* of about 6 K in the middle stratosphere and about 1 K in the mid-latitude lower stratosphere. Heat budget and radiative calculations show that these statistically significant warming regions result primarily from a dynamically induced enhancement of the residual meridional circulation, due to the presence of the dramatically reduced polar ozone. Later in the year (January–March), the reduced ozone values have spread meridionally across the Southern Hemisphere, producing widespread cooling of about 1–1.5 K. Consistent with this, the Southern Hemisphere mean lower stratospheric cooling averages nearly 1°C, roughly in agreement with the observational analysis of Oort and Liu (1993).

The model exhibits substantial, but not dominant, dynamical (altered circulation) responses to the presence of the reduced polar ozone. The model also shows a tightening of the polar vortex and thus resistance to export of its depleted ozone to lower latitudes. These results predict that, in accordance with the mechanistic model of Mahlman et al. (1986), the springtime meridional slopes of quasi-conservative tracer isolines will be *steepened* relative to their climatological positions. Thus, the entire springtime transport climatology of the Southern Hemisphere lower stratosphere should be altered by the onset of the Antarctic ozone hole phenomenon. Over the entire year, however, the impact of the altered circulation lessens considerably, thus remaining consistent with the tentative conclusion of IPCC (1992) that radiation-only calculations of ozone hole effects are a useful approximation.

Although this is a more ambitious step than those previously attempted, experiments such as these need to be conducted with better photochemistry, higher model resolution with improved model physics, and longer model interval runs. The model ozone destruction parameterization was designed for the Northern Hemisphere to participate, but its response was negligible, thus exposing a major limitation of this model experiment. The model calculations are suggestive of upper-troposphere cooling being produced by the Antarctic ozone losses. However, the magnitudes are too small to be judged statistically significant in this short model run. This simulation also suggests significant alteration to the budget of tropospheric ozone through substantial decreases in spring downward transport across the Southern Hemisphere tropopause. These questions need to be addressed in greater detail in subsequent studies.

Acknowledgments. The authors are indebted to the Computer Operations staff of GFDL for their excellent support and patience during the extended period required to complete these model experiments and to the Scientific Illustration group and Ms. Wendy Marshall of GFDL for their technical support. The perceptive criticisms and comments by Drs. Marvin Geller, Lori Perliski, V. Ramaswamy, Keith Shine, and an anonymous reviewer are gratefully acknowledged.

We dedicate this paper to the memory of the late Dr. Stephen Fels. It was his pioneering leadership in radiative–dynamical interaction that exposed us to the possibilities for this research.

REFERENCES

Allen, M., and J. E. Frederick, 1982: Effective photodissociation cross sections for molecular oxygen and nitric oxide in the Schumann–Runge bands. *J. Atmos. Sci.*, **39,** 2066–2075.

Anderson, J. G., W. H. Brune, and M. J. Proffitt, 1989: Ozone destruction by chlorine radicals within the Antarctic vortex: The spatial and temporal evolution of ClO–O_3 anticorrelation based on in situ ER-2 data. *J. Geophys. Res.*, **94,** 11 465–11 479.

Barrett, J. W., P. M. Solomon, R. L. de Zafra, M. Jaramillo, L. Emmons, and A. Parish, 1988: Formation of the Antarctic ozone hole by the ClO dimer mechanism. *Nature*, **336,** 455–458.

Cariolle, D., A. Lasserre-Bigorry, J. F. Royer, and J. F. Geleyn, 1990: A general circulation model simulation of the springtime Antarctic ozone decrease and its impact on mid-latitudes. *J. Geophys. Res.*, **95,** 1883–1898.

Crutzen, P. J., and F. Arnold, 1986: Nitric acid cloud formation in the cold Antarctic stratosphere: A major cause for the springtime "Ozone Hole." *Nature*, **332,** 651–655.

Farman, J. C., B. G. Gardiner, and J. D. Shanklin, 1985: Large losses of total ozone in Antarctica reveal seasonal ClO_x/NO_x interactions. *Nature*, **315,** 207–210.

Fels, S. B., and L. D. Kaplan, 1975: A test of the role of longwave radiative transfer in a general circulation model. *J. Atmos. Sci.*, **33,** 779–789.

——, J. D. Mahlman, M. D. Schwarzkopf, and R. W. Sinclair, 1980: Stratospheric sensitivity to perturbations in ozone and carbon dioxide: Radiative and dynamical response. *J. Atmos. Sci.*, **38,** 2265–2297.

Hartmann, D. L., 1976a: The structure of the stratosphere in the Southern Hemisphere during late winter 1973 as observed by satellite. *J. Atmos. Sci.*, **33,** 1141–1154.

——, 1976b: The dynamical climatology of the stratosphere in the Southern Hemisphere during late winter 1973. *J. Atmos. Sci.*, **33,** 1789–1802.

Hayashi, Y., D. G. Golder, J. D. Mahlman, and S. Miyahara, 1989: The effect of horizontal resolution on gravity waves simulated by the GFDL "SKYHI" general circulation model. *Pure Appl. Geophys.*, **130,** 421–443.

Hofmann, D. J., and S. Solomon, 1989: Ozone destruction through heterogeneous chemistry following the eruption of El Chichon. *J. Geophys. Res.*, **94,** 5029–5041.

Intergovernmental Panel on Climate Change, 1992: *The Supplementary Report to the IPCC Scientific Assessment.* J. T. Houghton, B. A. Callander, and S. K. Varney, Eds., Cambridge University Press, 200 pp.

Jenouvrier, A., B. Coquart, and M. F. Merienne-LaFore, 1986: New measurements of the absorption cross sections in the Herzberg continuum of molecular oxygen in the region between 205 and 240 nm. *Planet Space Sci.*, **34,** 253–254.

Juckes, M. N., and M. E. McIntyre, 1987: A high resolution one-layer model of breaking planetary waves in the stratosphere. *Nature*, **328,** 590–596.

Kiehl, J. T., B. A. Boville, and B. P. Brieglieb, 1988: Response of a general circulation model to a prescribed Antarctic ozone hole. *Nature*, **332,** 501–504.

Mahlman, J. D., and S. B. Fels, 1986: Antarctic ozone decreases: A dynamical cause? *Geophys. Res. Lett.*, **13,** 1316–1319.

——, and L. J. Umscheid, 1987: Comprehensive modeling of the middle atmosphere: The influence of horizontal resolution.

Transport Processes in the Middle Atmosphere, G. Visconti and R. Garcia, Eds., D. Reidel, 251–266.

——, H. Levy II, and W. J. Moxim, 1986: Three-dimensional simulations of stratospheric N_2O: Predictions for other trace constituents. *J. Geophys. Res.*, **91**(D2), 2687–2707.

Oort, A. H., and H.-Z. Liu, 1993: Upper air temperature trends over the globe, 1958–1989. *J. Climate*, **6**, 292–307.

Prather, M. J., M. M. Garcia, R. Suozzo, and D. Rind, 1990: Global impact of the Antarctic ozone hole: Dynamical dilution with a three-dimensional chemical transport model. *J. Geophys. Res.*, **95**, 3449–3471.

Ramaswamy, V., M. D. Schwarzkopf, and K. P. Shine, 1992: Radiative forcing of climate from halocarbon-induced global stratospheric ozone loss. *Nature*, **355**, 810–812.

Randel, W. J., 1987: Global Atmospheric Circulation Statistics, 1000–1 mb. NCAR Tech. Note NCAR/TN-295+STR, National Center for Atmospheric Research, 245 pp.

Shine, K. P., 1986: On the modeled thermal response of the Antarctic stratosphere to a depletion of ozone. *Geophys. Res. Lett.*, **13**, 1331–1334.

Solomon, S., 1990: Antarctic ozone: Progress toward a quantitative understanding. *Nature*, **347**, 347–354.

Stolarski, R. S., P. Bloomfield, R. D. McPeters, and J. R. Herman, 1991: Total ozone trends deduced from *Nimbus-7* TOMS data. *Geophys. Res. Lett.*, **18**, 1015–1018.

Toon, O. B., P. Hamill, R. P. Turco, and J. Pinto, 1986: Condensation of HNO_3 and HCl in the winter polar stratospheres. *Geophys. Res. Lett.*, **13**, 1284–1287.